

A Two-Subband Self-Consistent Model for High Electron Mobility Transistor Including Intersubband and Intraband Scattering Mechanisms *

R. Khoie, and H. Arman
 Department of Electrical and Computer Engineering
 University of Nevada, Las Vegas
 Las Vegas, NV 89154

Abstract

A new two dimensional numerical model for $Al_xGa_{1-x}As/GaAs$ High Electron Mobility Transistor with multisubband transport in the quantum well is presented. We previously extended the work of Widiger¹ and reported a *one-subband* self-consistent Schrodinger-Poisson solver^{2,3} in a two-dimensional numerical model for HEMT. In this paper we extend our previous model to a *two-subband* self-consistent model. We have incorporated an additional self-consistency by calculating the field-dependent, energy-dependent scattering rates due to ionized impurities and polar optical phonons for up to five subbands in the quantum well. These scattering rates are in good agreement with those reported by Yokoyama and Hess⁴ and are reported elsewhere in this Proceedings.⁵

The two higher moments of Boltzmann Transport Equation are numerically solved for the two lowest subbands and the bulk system; six transport equations, four for the two subbands and two for the bulk system. The Schrodinger and Poisson Equations are also solved self-consistently. The wavefunctions obtained are used to calculate the ionized impurity scattering and the polar optical phonon scattering rates for five lowest subbands in the quantum well. The rates of transfer of electrons and their energies to and from each subband are calculated from these intersubband and intrasubband scattering rates. In this model we consider the electrons in the lowest *two subbands* to be in the quantum well forming the 2-dimensional electron gas, and the electrons in the third and higher subbands to behave as bulk electrons with no restrictions in their motion.

I. Introduction

Yokoyama and Hess⁴ reported that at 77°K, 98 percent of electrons in the quantum well reside in the lowest subband whereas at 300°K, the population of electrons residing in the lowest subband reduces to 68 percent. In fact, at 300°K close to 18 percent of electrons in the quantum well reside in the second subband with their motion restricted to two dimensions. Widiger¹ reported a hydrodynamic transport model consisting of the two higher moments of Boltzmann Transport Equation (BTE) for

*This research was supported by the U.S. Army Research Office under ARO Grant No. DAAL 03-87-G-0004

¹D. J. Widiger, I. C. Kizilyalli, K. Hess, and J. J. Coleman, *IEEE Trans. on Electron Devices*, Vol. 32, No. 6, pp. 1092-1102, June 1985.

²Z. H. Ng, and R. Khoie, *IEEE Trans. on Electron Devices*, Vol. 38, No. 4, pp. 852-861, April 1991.

³Z. H. Ng, and R. Khoie, *Computational Electronics, Semiconductor Transport and Device Simulation*, edited by: K. Hess, J. P. Leburton, and U. Ravaioli, Kluwer Academic, pp. 55-58, January 1991.

⁴K. Yokoyama and K. Hess, *Phys. Rev. B* Vol. 33, pp. 5595-5606, 1986.

⁵H. Arman, and R. Khoie, *Elsewhere in this Proceedings*, May 1992.

a HEMT structure in which the quantum well was treated by using a triangular well approximation. Widiger's model considered only the lowest subband in the quantum well and assumed that a group of closely spaced second and higher subbands have the property of a bulk system. We previously reported^{2,3} a two-dimensional self-consistent numerical model for HEMT in which the quantization of electrons in the quantum well was taken into account by solving Schrodinger and Poisson Equations self-consistently. In that model, however, we assumed that only the electrons in the first subband were quantized, and that the electrons in the second and higher subbands behave as bulk electrons with no dimensional restriction in their motion. This assumption, particularly at 300°K, in light of the fact that only 68 percent of electrons reside in the first subband, is not valid.

In this work, we extend our previous One-Subband Self-Consistent Boltzmann Transport Equation (OS-SCBTE)^{2,3} model to a Multi-Subband Self-Consistent Boltzmann Transport Equation (MS-SCBTE) model. The two higher moments of Boltzmann Transport Equation are numerically solved for the two lowest subbands and the bulk system; six transport equations, four for the two subbands and two for the bulk system. The Schrodinger and Poisson Equations are also solved self-consistently. The wavefunctions obtained are used to calculate the ionized impurity scattering and the polar optical phonon scattering rates for five lowest subbands in the quantum well. The rates of transfer of electrons and their energies to and from each subband are calculated from these intersubband and intrasubband scattering rates. In this model we consider the electrons in the lowest *two subbands* to be in the quantum well forming the 2-dimensional electron gas, and the electrons in the third and higher subbands to behave as bulk electrons with no restrictions in their motion.

II. Basic System of Equations

The Poisson Equation² is given by:

$$\frac{\partial^2 V}{\partial x^2} + \frac{\partial^2 V}{\partial y^2} = -\frac{q}{\epsilon}[N_D(x, y) - n(x, y)] \quad (1)$$

where q is the electronic charge, ϵ the dielectric constant, n the total electron concentration, and N_D the donor doping level. The Schrodinger Equation is given by:

$$-\frac{\hbar^2}{2m^*} \frac{d^2 \psi_i(x)}{dx^2} - qV(x, y)\psi_i(x) = E_i \psi_i(x) \quad (2)$$

where m^* is the electron effective mass, $V(x, y)$ the electrostatic potential, and ψ_i the wavefunction corresponding to the eigenenergy E_i for the i -th subband.

The two higher moments of BTE: the particle conservation equation, and the energy conservation equation for the i -th subband of the one-dimensional quantum well are given by:

$$\frac{\partial(n_i(x, t))}{\partial t} = \nabla \cdot (-\mu_i n_i(x, t) \nabla V(x) + \nabla(D_i n_i(x, t))) + \sum_{j \neq i} \left(\frac{n_j - n_{oj}}{\tau_{ji}} \right) - \sum_{j \neq i} \left(\frac{n_i - n_{oi}}{\tau_{ij}} \right) \quad i = 1, 2 \quad (3)$$

$$\frac{\partial(n_i(x, t) E_i(x, t))}{\partial t} = -J \cdot \nabla V(x) + \nabla \cdot (-\mu_{E,i} n_i(x, t) E_i(x, t) \nabla V(x) + \nabla(D_{E,i} n_i(x, t) E_i(x, t))) \quad (4)$$

$$+ \sum_{j \neq i} \left(\frac{n_j E_j - n_{jo} E_{oj}}{\tau_{E,ji}} \right) - \sum_{j \neq i} \left(\frac{n_i E_i - n_{io} E_{io}}{\tau_{E,ij}} \right) - \sum_{j \neq i} \left(\frac{n_i - n_{oi}}{\tau_{ji}} \right) \hbar \omega_0 \quad i = 1, 2$$

In these equations n and J are the electron concentration and current, respectively. μ_i , D_i , $\mu_{E,i}$, and $D_{E,i}$ are the mobility, and diffusivity of carriers, and energy flux, respectively. E is the average

electron energy, and τ_{ij} , and $\tau_{E,ij}$ are relaxation times for carriers and their energies, respectively. $\hbar\omega_0$ is the polar optical-phonon energy. The first four summation terms (e.g.: $\sum_{j \neq i} (\frac{n_j - n_{oj}}{\tau_{ji}})$) in Eqs. (3) and (4) account for the rate of transfer of electrons and their energies to and from each subband. The last summation term ($-\sum_{j \neq i} (\frac{n_j - n_{oj}}{\tau_{ji}}) \hbar\omega_0$), in Eq. (4) accounts for the loss of energy by the electron to the polar optical-phonon. The details of the calculation of these scattering relaxation times are reported elsewhere in this Proceedings.⁵

In the bulk (electrons in the third and higher subbands), the two higher moments of BTE are:

$$\frac{\partial n}{\partial t} = \nabla \cdot (-\mu n \nabla V + \nabla(Dn)) + G_i \quad i = 1, 2 \quad (5)$$

$$\frac{\partial(nE)}{\partial t} = -J \cdot \nabla V - nB + \nabla \cdot \alpha(-\mu n E \nabla V + \nabla(DnE)) + F_i \quad i = 1, 2 \quad (6)$$

where B is the energy dissipation factor, α is the ratio of μ to μ_E . The term G_i is a generation like term that takes into account the transfer of electrons between the bulk and the first ($i=1$) and second ($i=2$) subbands. The term F_i is a similar term that takes the rate of energy transfer between the bulk and the two subbands into account.

III. Results and Conclusions

The structure of the HEMT device used in our simulations is shown in Fig. (1a). The doping level of GaAs is 10^{14} cm^{-3} , and the doping level of AlGaAs is $5.0 \times 10^{17} \text{ cm}^{-3}$. The $i_d - v_{ds}$ characteristics of the device for three different gate biasing conditions: $V_g = 0.45 \text{ V}$, 0.5 V , and 0.7 V are shown in Fig. (1b). Also shown are those calculated by the OS-SCBTE model. In both cases, the slopes of the $i - v$ curves decrease as the drain voltage increases, but the MS-SCBTE model predicts lower drain currents. This is due to the inclusion of the scattering rates in the transport of electrons which tends to reduce the electron concentration in the quantum well. With a gate bias of 0.7 V the MS-SCBTE model predicts that the onset of saturation in the drain current is about 0.8 V , whereas by prediction of OS-SCBTE model the onset of saturation occurs at around 1.2 V .

The electron concentration in the first subband, second subband, and the bulk are shown in Fig (2). At 300°K , about 72 percent of electrons are in the first subband and 26 percent are in the second subband. These results agree with those reported by Yokoyama and Hess⁴. Our results show the significance of the contribution of the scattering of the electrons in the second subband to the channel conductance. The values of transconductance, gate capacitance, and unity gain frequency under various gate voltages are shown in Fig. (3), along with the results obtained from the previous OS-SCBTE model. It has been reported⁶ that the transconductance increases with the gate voltage at low voltage levels, and then decreases as the gate voltage is further increased. This effect was not shown by the OS-SCBTE model, instead, the transconductance decreased linearly with the gate voltage. Similar behavior is observed in the unity gain frequency characteristics. With the present model, we obtained lower transconductance and unity gain frequency which were overestimated in the previous model. At a gate bias of 0.625 V , we obtained a transconductance of 316 mS/mm , a gate capacitance of 17.68 pF/cm , and a unity-gain frequency of 28.44 GHz , compared to the transconductance of 520 mS/mm , the gate capacitance of 21.0 pF/cm , and the unity gain frequency of 39 GHz , reported earlier.²

⁶D. Loret, *Solid-State Electronics*, Vol. 30, pp. 1197-1203, 1987.

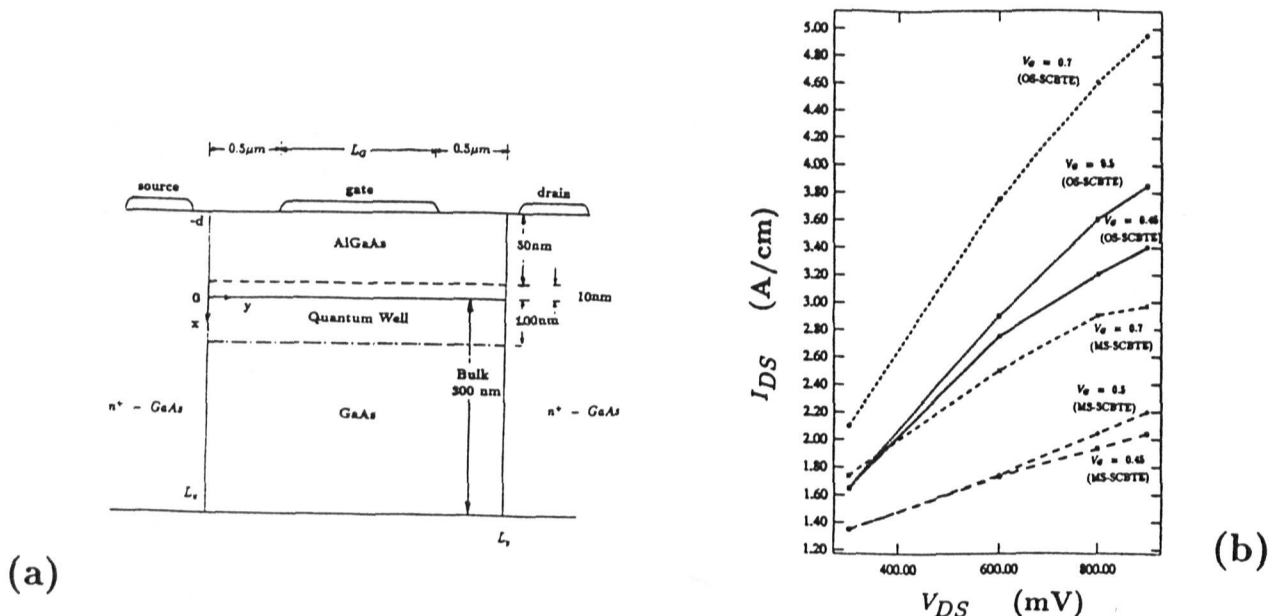


Figure 1: (a) HEMT device simulated, (b) $i_d - v_{ds}$.

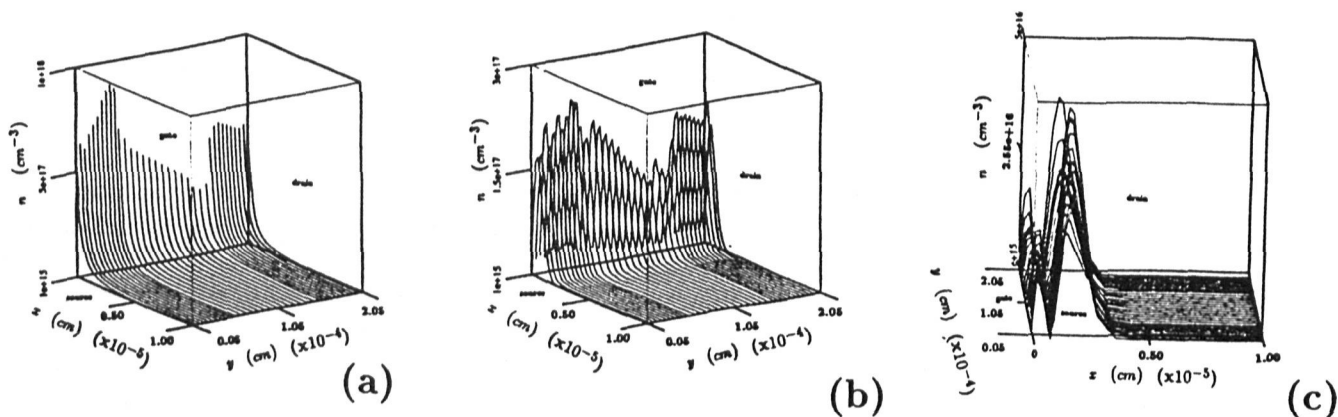


Figure 2: Electron density in (a) bulk, (b) first and (c) second subband: $v_g = 0.7 \text{ V}$ and $v_{ds} = 0.5 \text{ V}$.

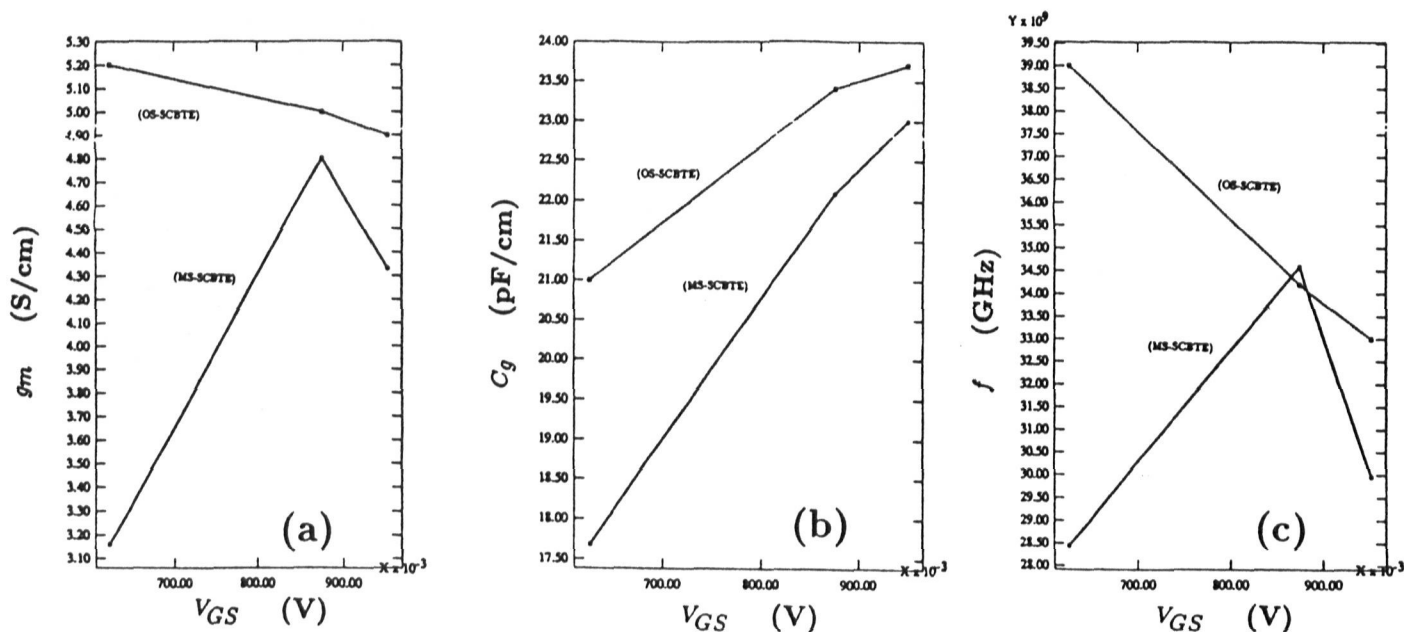


Figure 3: a) Transconductance, (b) gate capacitance, and (c) unity gain frequency: $v_{ds} = 1.0 \text{ V}$.